Amino Acids (2012) 43:207–218
DOI 10.1007/s00726-011-1065-1

ORIGINAL ARTICLE

Design, conformational studies and analysis of structure–function relationships of PTH (1–11) analogues: the essential role of Val in position 2

A. Caporale · L. Gesiot · M. Sturlese · A. Wittelsberger · S. Mammi · E. Peggion

Received: 27 June 2011 / Accepted: 24 August 2011 / Published online: 15 September 2011

Abstract The N-terminal 1–34 segment of parathyroid hormone (PTH) is fully active in vitro and in vivo and it elicits all the biological responses characteristic of the native intact PTH. Recent studies reported potent helical analogues of the PTH (1–11) with helicity-enhancing substitutions. This work describes the synthesis, biological activity, and conformational studies of analogues obtained from the most active non-natural PTH (1–11) peptide H-Aib-Val-Aib-Glu-Ile-Gln-Leu-Nle-His-Gln-Har-NH_2; specifically, the replacement of Val in position 2 with D-Val, L-(αMe)-Val and *N*-isopropyl-Gly was studied. The synthesized analogues were characterized functionally by in-cell assays and their structures were determined by CD and NMR spectroscopy. To clarify the relationship between the structure and activity, the structural data were used to generate a pharmacophoric model, obtained overlapping all the analogues. This model underlines the fundamental functional role of the side chain of Val^2 and, at the same time, reveals that the introduction of conformationally constrained C^{α}-tetrasubstituted α-amino acids in the peptides increases their helical content, but does not necessarily ensure significant biological activity.

Keywords PTH · NMR analysis · Pharmacophoric model · αMeVal · Conformational analogues · Structure/activity analysis

Abbreviations

Aib	α-Aminoisobutyric acid
CD	Circular dichroism
DIPEA	*N*,*N*-Diisopropylethylamine
DMF	*N*,*N*-Dimethylformamide
EDT	Ethanedithiol
Har	Homoarginine
HATU	1-[Bis(dimethylamino)methylene]-1*H*-7-azabenzotriazolium hexafluorophosphate 3-oxide
HBTU	1-[Bis(dimethylamino)methylene]-1*H*-benzotriazolium hexafluorophosphate 3-oxide
HOAt	1-Hydroxy-7-azabenzotriazole
HOBt	1-Hydroxybenzotriazole
Nle	Norleucine
NMP	*N*-Methyl-2-pyrrolidone
Nval	*N*-Isopropylglycine
PTH	Parathyroid hormone
TFA	Trifluoroacetic acid
TFE	2,2,2-trifluoroethanol
TIS	Triisopropylsilane
TMS	Trimethylsilane

Introduction

Parathyroid hormone (PTH), an 84-amino acid peptide hormone, plays a vital role in regulating calcium and

A. Caporale and L. Gesiot contributed equally to this work.

Electronic supplementary material The online version of this article (doi:10.1007/s00726-011-1065-1) contains supplementary material, which is available to authorized users.

A. Caporale (✉)
Department of Molecular Sciences and Nanosystems, Università Ca' Foscari di Venezia, Dorsoduro, 2137, 30123 Venice, Italy
e-mail: caporaleandrea74@gmail.com

L. Gesiot · M. Sturlese · S. Mammi · E. Peggion
Department of Chemical Sciences, Institute of Biomolecular Chemistry, CNR, University of Padova, via Marzolo 1, 35131 Padova, Italy

A. Wittelsberger
Department of Physiology, Tufts University School of Medicine, 136 Harrison Avenue, Boston, MA 02111, USA

phosphate homeostasis in mammalian blood. PTH-related protein (PTHrP) also plays a critical role in the development of the fetal skeleton (Kronenberg et al. 1997). The biological actions of both these peptides are mediated by the same G-protein-coupled receptor (GPCR) (Kolakowski 1994), the PTH/PTHrP receptor (PTH1R) (Jüppner et al. 1991). It has been shown that the first 34-amino acids of PTH are sufficient for in vivo bioactivity and to reproduce the biological responses characteristic of the native intact PTH (Kronenberg et al. 1997). Clinical studies have demonstrated that PTH (1–34) is a powerful bone anabolic agent, able to restore bone mineral density (Shimizu et al. 2001b; Barazza et al. 2005). NMR analysis of PTH (1–34) analogues has led to the conclusion that a short α-helical segment at the N terminus is necessary for the receptor activation. In addition, a more stable C-terminal α-helical segment is present. These two helices are separated by two hinge motifs located around positions 12 and 19 (Scian et al. 2006). According to the description, the interaction of PTH (1–34) with the receptor has been postulated to follow a "two-domain" model: the C-terminal portion interacts with the N-terminal extracellular domain of the receptor and then the N-terminal portion interacts with the PTH1R domain embedded in the membrane and elicits the cellular response (Hoare et al. 2001; Gardella and Jüppner 2001; Shimizu et al. 2002, 2005; Castro et al. 2005; Gensure et al. 2005; Wittelsberger et al. 2006; Dean et al. 2008; Pioszak et al. 2009; Vilardaga et al. 2011).

Studies to reduce the length of the active peptide have demonstrated that enhancement of α-helicity in the PTH (1–11) sequence results in potent PTH (1–11) NH_2 analogues (Tsomaia et al. 2004; Barazza et al. 2005; Potts and Gardella 2008). Mutagenesis investigations and molecular dynamics analysis suggested the co-localization of residue 8 (Met or Nle), Ile^5 and Val^2 on the same face of the helical N-terminal portion. This pattern is thought to be a fundamental requirement for the activation of the PTH1R receptor (Shimizu et al. 2000; Monticelli et al. 2002).

Introduction of conformational constraints, such as α-aminoisobutyric acid (Aib), into peptides, improves their activity and receptor binding selectivity (Hirschmann 1991; Gante 1994; Kessler et al. 1995; Caporale et al. 2010a). While alanine is easily accommodated in both folded and extended structures, theoretical and experimental studies performed on Aib (Kaul and Balaram 1999; Toniolo et al. 2001; Torras et al. 2008; Maity and König 2008) have highlighted its strong tendency to induce folded structures in the 3_{10}-/α-helical region (φ, $\psi \approx \pm 60°, \pm 30°$). On the contrary, semi-extended or fully-extended conformations are extremely rare for this residue. For N-terminal analogues of PTH containing Aib, such as H-[$Aib^{1,3}$, Gln^{10}, Har^{11}, Ala^{12}, Trp^{14}]-PTH (1–14)-NH_2 and H-[$Aib^{1,3}$, Gln^{10}, Har^{11}]-PTH (1–11)-NH_2, the helical contents determined by circular dichroism spectroscopy were shown to correlate with potencies, the EC_{50} values being 1.1 and 4.0 nM, respectively (Shimizu et al. 2001a).

Some modifications recently introduced in position 2, such as a D-Val residue (Caporale et al. 2009a), reduce or annihilate the activity of the most active PTH (1–11) analogue, H-Aib-Val-Aib-Glu-Ile-Gln-Leu-Nle-His-Gln-Har-NH_2 (**I**). We interpreted this behaviour as the consequence of an unsuitable orientation of the Val side chain, rather than of an overall 3-D structural alteration caused by the presence of non-proteinogenic amino acids. To investigate the role of Val^2, which is predicted to interact with Met^{425} at the extracellular end of the receptor (Gensure et al. 2005), we synthesized a series of analogues of **I** containing sterically hindered, helix-promoting C^{α}-tetrasubstituted amino acids (Shimizu et al. 2001b; Crisma et al. 2002) (Table 1) and characterized them both conformationally and biologically.

Our research approach (Scian et al. 2006; Caporale et al. 2009a) is aimed at the definition of the pharmacophoric moieties and tries to define the critical residues in the N-terminal PTH (1–11) segment. For this purpose, we decided to use both active and completely inactive analogues containing residues mimicking Val in position 2. The sensitive role of Val^2 has been demonstrated by the potency decrease due to the simple modification of the side chain orientation (Caporale et al. 2009a). In this work, a CD and 2-D NMR conformational analysis was performed on the most relevant analogues synthesized. The solution structures were determined using a distance-restrained molecular dynamics approach, based on nuclear Overhauser enhancement data. The conformations were compared with the known solution structure of the reference peptide **I** (Caporale et al. 2009a). Finally, all peptides were tested in vitro to determine their potency.

Materials and methods

Synthesis

General

Starting materials were obtained from commercial suppliers and used without further purification. Rink Amide MHBA Resin (0.73 mmol/g loading) as a solid support was obtained from Inalco-Novabiochem (Milano, Italy). HOBT, HBTU, and Fmoc-protected natural amino acids were obtained from GL Biochem (Shangai, China). Cyanuric fluoride was purchased from Lancaster (Morecambe, England). Fmoc-Aib-OH was purchased from NeoMPs (Strasbourg, France). Only D-Har was synthesised as previously reported (Caporale et al. 2009b). DMF dried over molecular

Table 1 Analogues of PTH (1–11) containing sterically hindered, helix-promoting, C^{α}-tetrasubstituted amino acids

Entry	Peptide	Chemical formula	MW^{a}_{Calc}	$[M + H]^{+}$ found	R_t (min)[b]
I	H-Aib-Val-Aib-Glu-Ile-Gln-Leu-Nle-His-Gln-Har-NH_2	$C_{59}H_{103}N_{19}O_{15}$	1,317.74	1,318.25	16.98
II	H-Aib-DVal-Aib-Glu-Ile-Gln-Leu-Nle-His-Gln-Har-NH_2	$C_{59}H_{103}N_{19}O^{c}_{15}$	1,317.74	1,318.24	16.90
III	H-Ala-Nval-Aib-Glu-Ile-Gln-Leu-Nle-His-Gln-Har-NH_2	$C_{58}H_{101}N_{19}O^{d}_{15}$	1,303.74	1,304.46	16.34
IV	H-D-Har-D-Gln-D-His-D-Nle-D-Leu-D-Gln-D-Ile-D-Glu-Aib-D-Val-Aib-NH_2	$C_{59}H_{103}N_{19}O^{c}_{15}$	1,317.74	1,318.47	17.82
V	H-Aib-(αMe)Val-Ser-Glu-Ile-Gln-Leu-Nle-His-Asn-Arg-NH_2	$C_{57}H_{99}N_{19}O_{16}$	1,306.54	1,307.43	16.40
VI	H-Ala-(αMe)Val-Ser-Aib-Ile-Gln-Leu-Nle-His-Asn-Arg-NH_2	$C_{55}H_{97}N_{19}O_{14}$	1,247.71	1,248.59	16.72
VII	H-Ala-(αMe)Val-Aib-Glu-Ile-Gln-Leu-Nle-His-Asn-Arg-NH_2	$C_{57}H_{99}N_{19}O_{15}$	1,289.73	1,290.57	16.81
VIII	H-Aib-(αMe)Val-Aib-Glu-Ile-Gln-Leu-Nle-His-Asn-Arg-NH_2	$C_{58}H_{101}N_{19}O_{15}$	1,303.74	1,304.46	17.23
IX	H-Aib-(αMe)Val-Aib-Glu-Ile-Gln-Leu-Nle-His-Gln-Har-NH_2	$C_{60}H_{105}N_{19}O_{15}$	1,331.74	1,332.65	17.36
X	H-Ac_5c-(αMe)Val-Aib-Glu-Ile-Gln-Leu-Nle-His-Gln-Har-NH_2	$C_{62}H_{107}N_{19}O_{15}$	1,357.74	1,359.69	18.16
XI	H-Ac_5c-Val-Aib-Glu-Ile-Gln-Leu-Met-His-Gln-Arg-NH_2	$C_{59}H_{101}N_{19}O_{15}S$[e]	1347.70	1,348.49	16.76

[a] Monoisotopic molecular weight calculated from the chemical formula

[b] R_t was determined with a linear gradient of 10–90% (v/v) B over 30 min (A: water + 0.1% TFA; B: 90% acetonitrile + 0.1% TFA) using a Vydac C18 column (218TP510)

[c] (Caporale et al. 2009a)

[d] (Caporale et al. 2010b)

[e] (Barazza et al. 2005)

sieves ($H_2O < 0.01\%$) and DIPEA was purchased from Fluka (Buchs, Switzerland). Dry dichloromethane was distilled from P_2O_5 and kept over 4 Å molecular sieves. Water for reversed-phase high performance liquid chromatography (HPLC) was filtered through a 0.22 μm Millipak40 membrane filter (Millipore, Billerica, MA, USA). Reversed-phase purification was routinely performed on a Shimadzu LC-8A equipped with a Shimadzu SPD-6A UV detector on a Deltapak Waters C_{18}-100Å silica HPLC column. The operative flow rate was 17 ml/min with a linear gradient of 20–45% (v/v) B over 20 min (A: water + 0.1% TFA; B: 90% acetonitrile + 0.1% TFA). Homogeneity of the products was assessed by analytical reversed-phase HPLC using a Vydac C18 column (218TP510), with a linear gradient of 10–90% (v/v) B in 30 min, a flow rate of 1 ml/min and UV detection at 214 nm. Molecular masses of the final peptides were determined with a Perseptive Biosystems MARINER™ API-TOF spectrometer (Framingham, MA, USA).

Solid-phase peptide synthesis

Fmoc-protected Rink Amide MHBA Resin (100 mg, 0.072 mmol) was swelled twice in DMF for 30 min each time and then it was treated with 20% piperidine in DMF (5 and then 25 min), and washed with DMF (Carpino et al. 1994). The first amino acid was anchored to the resin using the HBTU/HOBt/DIPEA protocol (Carpino and El-Faham 1994). Deprotection of Fmoc from the α-amino groups was achieved under standard conditions, with a 20% piperidine solution in DMF. The following amino acids were introduced similarly. The coupling of Aib and Val was accomplished with the more potent condensation reagent HATU (Carpino et al. 1995). To improve the incorporation yield of hindered amino acids, a longer reaction time and double couplings were used. The (αMe)Val residue was prepared as Fmoc-(αMe)Val-F; an excess of three eq. and one eq. of DIEA were used (Carpino et al. 1991) for 2 h and the procedure was repeated twice. The amino acid following (αMe)Val or other C^{α}-tetrasubstituted amino acids was introduced on the resin using the same protocol. The resin-bound peptides were treated with a deprotection and cleavage solution of TFA/TIS/water (95:2.5:2.5 v/v/v) at room temperature for 2 h, except for the peptide containing Met, for which the mixture TFA/EDT/TIS/water (94:2.5:1:2.5 v/v/v/v) was used. After filtration, the filtrate was concentrated under nitrogen and precipitated with methyl *tert*-butyl ether. Peptide purification was performed by reverse-phase HPLC. Molecular masses were determined by electrospray ionization mass spectrometry (ESI–MS).

Preparation of Fmoc-(αMe)Val-OH (Obrecht et al. 1995) Hundred milligrams of H-(αMe)Val-OH (0.76 mmol) was suspended in 4 ml of dry DCM under nitrogen atmosphere. One hundred and ninety microliters of TMS-Cl (1.52 mmol, 2 eq.) was added and the mixture was refluxed for 2 h. Then, a third eq. of TMS-Cl was added and reflux continued for 1 h. The mixture was then cooled to 0°C and 260 μl of DIEA (2.27 mmol, 3 eq.) and 196.6 mg of Fmoc-Cl (0.76 mmol, 1 eq.) were added. The reaction was

followed by TLC (chloroform:methanol 9:1 and light petroleum ether:ethyl acetate 7:3). The solvent was evaporated and the crude material was dissolved in 20 ml of water containing 10% $NaHCO_3$ and extracted with diethyl ether (3 times). The organic layers were retro-extracted with a solution of $NaHCO_3$ (10%). The water layers were acidified to pH 2 using conc. HCl, and extracted with ethyl acetate (5 times). Then, the organic layers were dried over Na_2SO_4. The solvent was evaporated to obtain yellowish oil which solidified slowly. The yield amounted to 88%. The MW was determined by mass spectrometry; the calculated and experimental masses were 354.4 and 354.2 [M + H^+], respectively. ^{1}H NMR (200 MHz) in $CDCl_3$: 7.9–7.5 ppm (8H Fmoc), 6.4 ppm [bm, 1H N*H*(amide)], 4.5 ppm [d, 2H CH_2(Fmoc)], 4.25–4.20 ppm [bm, 1H C*H*(Fmoc)], 2.10–2.00 ppm (t, 6H, 2 CH_3), 1.50 ppm (s, 3H), 1.1–0.9 [m, H, C*H*$(CH_3)_2$)].

Preparation of Fmoc-(αMe)Val-F Thiry-four microliters of pyridine (0.42 mmol, 1 eq.) and 72 µl of cyanuric fluoride (0.85 mmol, 2 eq.) were added to 150 mg of Fmoc-(αMe)Val-OH (0.42 mmol, 1 eq.) in 2 ml of DCM, at 0°C. The mixture was allowed to reach at room temperature and 3 h later it was extracted with water and ice (3 times). The organic layer was then washed with cold water and dried over Na_2SO_4. Then, the solvent was evaporated under vacuum. The purity of the product was confirmed by IR analysis (1,835 cm^{-1} (s C=O)) (Caporale et al. 2006).

Circular dichroism

Far UV–CD spectra were collected on a Jasco J-715 spectropolarimeter (Tokyo, Japan) controlled by a PC. The J-700 software was used to acquire and process the spectra. All experiments were performed at room temperature using Hellma quartz cells and optical path-lengths of 0.01 and 0.1 cm. Spectra were recorded using a bandwidth of 2 nm and a time constant of 8 s at a scan speed of 20 nm/min, in a wavelength range of 190–250 nm; the concentration of the peptides was in the range of 0.07–1.07 mM. The peptides were dissolved in aqueous solution containing 20% (v/v) TFE. The signal-to-noise ratio was improved by accumulating 8 scans. The helical content for each peptide was estimated according to the literature (Yang et al. 1986).

NMR measurements

NMR spectra were recorded at 298 K on a Bruker AVANCE DMX-600 spectrometer. The experiments were carried out in H_2O/TFE-d_3 (4:1) v/v. The sample concentration was ~1 mM in 600 µl of solution. The water signal was suppressed by pre-saturation during the relaxation delay. The spin systems of all amino acid residues were identified using standard DQF or magnitude-COSY (Rance et al. 1983) and CLEAN-TOCSY (Bax and Davis 1985a; Griesinger et al. 1988) spectra. In the latter case, the spin-lock pulse sequence was 70 ms long. The sequence-specific assignment was accomplished using the rotating-frame Overhauser enhancement spectroscopy (ROESY) (Bax and Davis 1985b), with a mixing time of 150 ms. All spectra were acquired by collecting 400–512 experiments, each one consisting of 32–256 scans and 4,096 data points. Spectral processing was carried out using XWINNMR. Spectra were calibrated against the TMS signal.

Molecular modelling

Simulated annealing (SA) calculations were carried out using the XPLOR-NIH 2.22 software. For distances involving equivalent or non-stereo-assigned protons, r^{-6} averaging was used. The molecular dynamics calculations involved a minimization stage of 100 cycles, followed by SA and a refinement stage. The SA consisted of 10,000 steps of dynamics at 1,500 K and of 15,000 steps of cooling from 1,500 to 100 K in 50 K decrements. The SA procedure was followed by 200 cycles of energy minimization. In the SA refinement stage, the system was cooled in 20,000 steps from 1,000 to 100 K in 50 K decrements. Finally, the calculations were completed with 200 cycles of energy minimization using a ROE force constant of 50 cal/(mole·Å). One hundred and fifty structures were generated for each analogue, and the ten minimum-energy structures containing no distance restraint violation were chosen for the conformational study. The secondary structure was determined using H-bond analysis (Baker and Hubbard 1984; Kabsch and Sander 1983) and the dihedral angle calculations using the MOE2008.10 and VMD 1.86 programs with a linux quadcore workstation.

The pharmacophoric model was developed with the MOE2008.10 software. It was built using the pharmacophore consensus utility and manually modified by the pharmacophore query editor. The ten minimum-energy structures of the reference analogue **I**, obtained from SA calculations, were included in the training set to build a primary model. The test set was composed of the ensemble of the other analogues. A set of ten features composes the final pharmacophoric model.

Activity assays

Human embryonic kidney (HEK 293) cells stably transfected with recombinant PTH1R receptor (HEK293/C20 cell line) were used (Pines et al. 1994). In HEK 293 cells, the cAMP response element (CRE) of luciferase was transfected using CRE-Luc plasmid. This response element

(CRE), which is a recognition site of certain transcription factors, interacts with CREB (CRE-binding protein), which is regulated by cAMP. Thus, the activity of PTH1R, which couples strongly to the adenylyl cyclase (AC)–protein kinase A (PKA) signalling pathway, is monitored by using CRE-positioned upstream of the luciferase gene. Activation of the receptor causes an increase in intracellular cAMP, which is able to activate protein kinase A to phosphorylate CREB. The luciferase concentration within cells is increased when phosphorylated CREB is bound to the CRE consensus sequence, causing an increase in transcription rate of the luciferase gene (Fan and Wood 2007).

Cell culture and CRE-Luc transfection

HEK293/C20 cell lines were cultured at 37°C in Dulbecco's modified Eagle's medium (DMEM) supplemented with 10% fetal bovine serum in a humidified atmosphere of 95% air and 5% CO_2. The cells were subcultured by treatment with Versene every week and the medium was changed every 3–4 days. Twenty-four hours before transfection, the cells were seeded at 10^5 cells/well in 24-well, collagen-coated plates. On the following day, the cells were treated with FuGENE 6 transfection reagent (1 µl/well), CRE-Luc plasmid (0.2 µg/well) in 0.5 ml/well Opti-Mem 1, serum free medium, according with the manufacturer's recommended procedure.

D-MEM, fetal bovine serum, Opti-Mem I, and PBS were purchased from Life Technologies, Inc. (Gaithersburg, MD, USA); FuGENE 6 transfection reagent was purchased from Roche Diagnostic (Indianapolis, IN, USA); passive lysis buffer, 5×, from Promega Corporation (Madison, WI, USA); Biocoat collagen I 24-well plates from Becton–Dickinson (Bedford, MA, USA), while the other tissue culture disposable and plastic ware were obtained from Corning (Corning, NY, USA). D-Luciferin potassium salt was obtained from Molecular Probes (Eugene, OR, USA).

Luciferase assay

About 18 h after CRE-Luc plasmid transfection, the cells were rinsed with PBS buffer and the transfection medium was replaced by 225 µl/well of DMEM. 25 µl/well of solutions of the various peptides at different concentrations (from 10^{-7} to 10^{-3}M, to obtain final concentrations between 10^{-8} and 10^{-4} M) in PBS, supplemented with 0.1% bovine serum albumin were then added to the wells and incubated at 37°C for 4.5 h, yielding maximal response to luciferase. After this time, the medium was aspirated and the cells were lysed by gentle shaking with 200 µl/well of passive lysis buffer. The cells were transferred to labelled low-binding Eppendorf tubes, centrifuged for 2 min, and 80 µl/tube of supernatant was transferred to individual sample glass tubes. Luciferase activity was measured using a Lumat LB 9507 luminometer (EG&G Berthold, Bad Wildbad, Germany). This instrument automatically injects defined volumes of two solutions, A and B, with the compositions described below. Initially, a solution 0, containing 25 mM glycylglycine, 15 mM $MgSO_4$ and 4 mM ethyleneglycol-bis (β-aminoethyl ether)-*N*,*N*,*N*′,*N*′-tetraacetic acid (EGTA) in deionized water, is prepared. Solution A has the same composition as Solution 0, with the addition of 0.2 mM D-luciferin. Solution B has the composition as same as Solution 0, with the addition of 0.02 M K_3PO_4, 2.5 mM ATP and 1 mM dithiothreitol. The instrument adds 100 µl of solution A and 300 µl of solution B to a sample tube, and performs the measurement for 20 s. All CRE-Luc experiments were carried out in triplicates.

Data calculations

Calculations and data analyses were performed using Microsoft Excel 2000 and GraphPad Prism, Version 3.0.

Results

All PTH (1–11) analogues were synthesized by SPPS employing the Fmoc amino acid protocol. During the synthesis, a combination of classical solid phase coupling reagents for proteinogenic amino acids and acyl fluoride derivatives for C^{α}-tetrasubstituted amino acids was used. In analogue **III**, Ala is present in position 1 instead of Aib to avoid steric hindrance with Nval in position 2. D-Har was synthesised with good purity and yield.

The activity was measured by the luciferase assay (Cali et al. 2008). The instrument response is correlated to the chemical concentrations of components of luciferase pathway reactions, so the light intensity can be used to associate an observable parameter with a molecular process. A general decrease of activity, except for analogue **XI**, was observed (Table 2). Analogues **I** (EC_{50} = 1.1 nM) and **II** ($EC_{50} = 7{\cdot}10^3$ nM) differ only for the chirality of Val^2, but their behaviour in terms of biological activity is very different, demonstrating the importance of the side chain orientation in χ space (Hruby et al. 1997) for biological activity.

The CD spectra were recorded under the same conditions used in the previous works for other PTH analogues (TFE/water 20:80 at 25°C) (Barazza et al. 2005; Caporale et al. 2009a, 2010a, b). No concentration dependence of the CD profiles was observed for any of these analogues (data not shown). Figure 1 shows the spectra of all analogues together with the spectrum of the reference peptide **I**.

To compare the CD spectra of retro-inverse analogue **IV** with those of the other peptides, its sign was changed. Even

Table 2 Biological activity of analogues of PTH (1–11)

Entry	EC_{50} (nM)
I	1.1
II	7,000
III	Not active
IV	Not active
V	Not active
VI	Not active
VII	Not active
VIII	700,000
IX	11,000
X	6,000
XI	14.3

EC_{50} is the result of the average of at least three experiments. EC_{50} is defined as the half-maximal effective concentration and is referred to the concentration of peptide which induces a response halfway between the baseline and the maximum

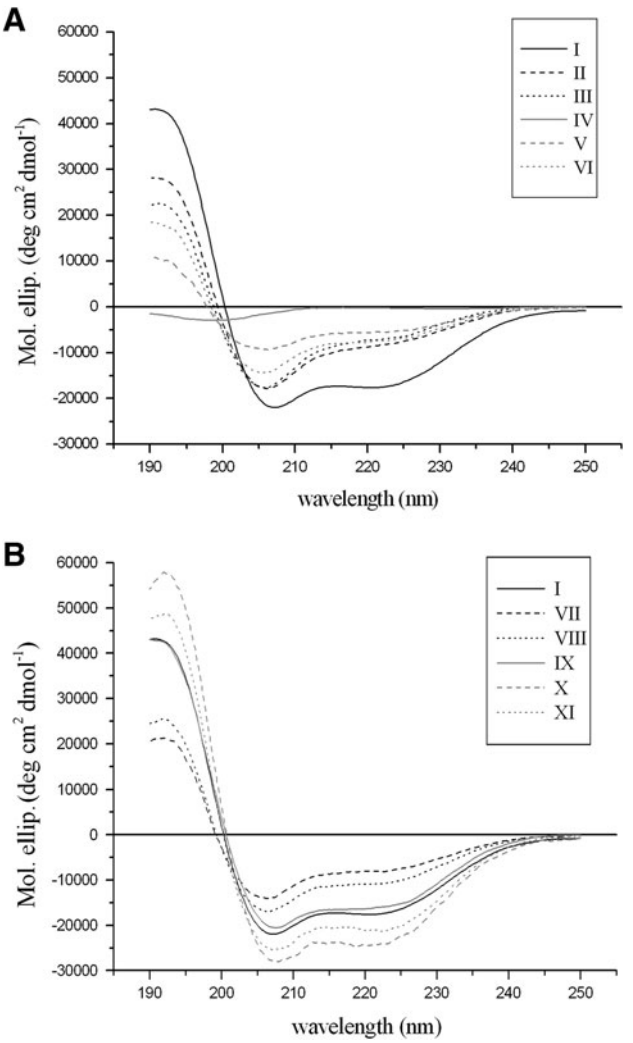

Fig. 1 CD spectra of all PTH (1–11) analogues described in this work. Spectra are reported in terms of mean residue molar ellipticity (deg cm^2 dmol^{-1}). Analogue **I** is reported in both spectra as internal reference

if analogue **IV** is apparently not related to the others, it partially helped to understand the role of the residue at position 2; it was particularly useful to evaluate the overall arrangement of the side chains and to further validate our pharmacophoric model. The spectrum of analogue **I** exhibits the typical shape of an α-helical conformation, with two negative bands of comparable magnitude near 222 and 208 nm, and a stronger positive band near 190 nm. Analogues **II** and **III** reveal an ordered structure, with a probable contribution of 3_{10}-helix or β-turn (Toniolo et al. 1996). For analogue **IV**, the ordered structure is very low or absent (Fig. 1a).

The introduction of the conformationally constrained C^{α}-tetrasubstituted amino acids (Toniolo et al. 2001; Maity and König 2008) in the sequence stabilizes the ordered structure of analogues from **V** to **X** (Fig. 1b); however, their spectrum is less intense than that of analogue **I**. The shape of these curves suggests a contribution of 3_{10} helix, in agreement with literature results (Moretto et al. 2008; Crisma et al. 2007), for CD of C^{α}-tetrasubstituted homopeptides (Fig. 1b).

1-Aminocyclopentane-1-carboxylic acid (Ac_5c) (Toniolo 1989; Crisma et al. 1988; Santini et al. 1988; Perczel et al. 1991; Willisch et al. 1991; Barazza et al. 2005) was introduced in analogue **X**. Ac_5c has a greater propensity to induce a helical conformation than Aib in the N-terminal position and this was confirmed by studies on the TOAC residue (Bui et al. 2000). As previously observed (Barazza et al. 2005), analogue **X** has a high α-helix content (Fig. 1b). Analogue **X** is more ordered and the two orders of magnitude are more potent than analogue **VIII**.

Complete proton resonance assignment was carried out using the standard procedure (Wüthrich 1986) (see Supplementary Information). The secondary chemical shifts can provide some important information on the structure of these analogues (Fig. 2).

The chemical shift differences of the αCH protons with respect to the corresponding random coil values identified a helical segment ($\delta\Delta < -0.1$ ppm), spanning the sequence from the first residue to the C-terminal zone. Such differences are bigger for the reference peptide, **I**, and for the analogues containing C^{α}-tetrasubstituted amino acids in position 1, 2 or 3. For most of the structured analogues, the ROESY spectra revealed the presence of αH(i)-HN(i + 3), αH(i)-βH(i + 3) and αH(i)-HN(i + 4) contacts, typical of the α-helix. The single substitution of the amino acid in position 3 or 4 with an Aib residue seemed to be more effective to promote helicity than the single substitution in

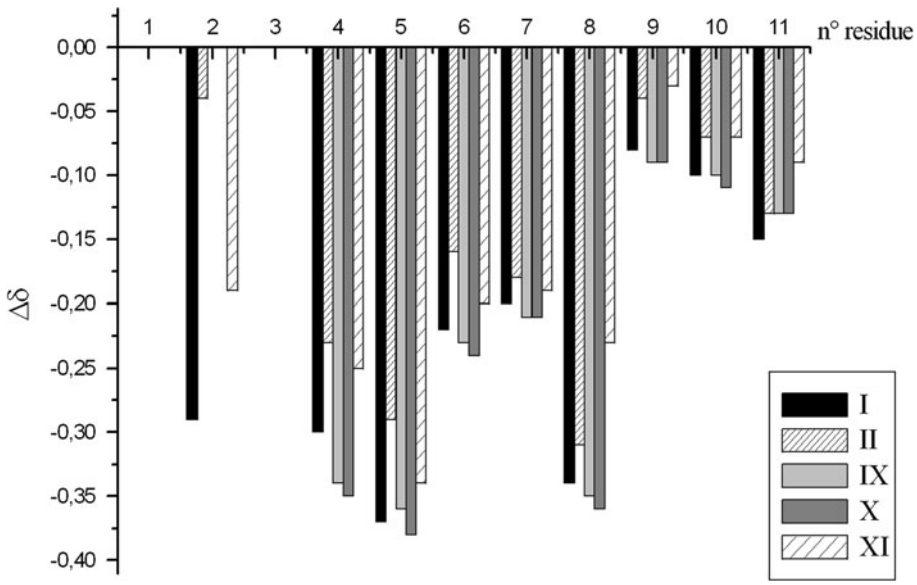

Fig. 2 The chemical shift differences between the αCH proton resonances ($\Delta\delta < -0.1$ ppm) and the corresponding random coil values identify a helical segment spanning the sequence from the first residue to the C-terminal zone (only the most potent analogues are reported here, see Figure S3 for a complete analysis)

position 1. For analogues **V**, **VI** and **VII** also the first residue appears comprised in the helical segment.

The structures were calculated using a simulated annealing (SA) protocol performed with Xplor-NIH 2.22. The ten lowest energy structures (out of 150) were selected for each analogue (Fig. 3). To analyze the secondary structure, Ramachandran plots were created with the MOE2008.10 package (See Figure S8 in the Supplementary Information). Each plot displays the φ, ψ pair of dihedral angles for each structure selected. The Ramachandran plot underlines the good agreement of the derived φ and ψ angles with a helical conformation for all analogues especially for the C-terminal segment from Glu^4 to Gln^{10}. Only for analogue **III**, several dihedral angles fall in less-favoured areas, because of the presence of the *N*-substituted glycine (see Figure S8 in the Supplementary Information).

To clarify the relationship between the structure and activity of the different analogues, the ensemble of structures of the reference peptide was used to generate a pharmacophoric model (Fig. 4). In principle, a high number of features can be considered, due to the number of atoms, roughly 200. The complexity of the model was reduced focusing on the nature and conformation of the side chains, and removing features related to Arg/Har11. Arginine or homoarginine was present in all analogues as the C-terminal residue, and the ROESY data suggested a wide conformational flexibility for this residue in every structure ensemble. On the contrary, the side chain conformations of the other residues were well defined, allowing a good description through a pharmacophoric model. The pattern of features included 10 sites: 6 hydrophobic, 2 donor/acceptor of hydrogen bonds, 1 anionic/acceptor, 1 aromatic/hydrophobic/acceptor/donor describing the imidazole ring. The analogues were well distinguished by the model: analogue **XI** shared the same pattern of analogue **I**; the analogues with moderate activity, i.e., **II**, **VIII**, **IX**, and **X**, showed a pattern similar to that of **I**, but with a higher RMDS (Table S5, Supplementary Information). The inactive analogues, such as **IV,** did not fit the pharmacophoric model.

Discussion

The replacement of natural amino acids with non-proteinogenic analogues, which are able to induce a defined secondary structure also in short peptides, is a way to obtain a more stable structure in solution. The introduction of conformational constraints might lock the peptide in its bioactive or catalytically active conformation. An additional advantage might be an increase of the peptide metabolic stability, and therefore its bio-availability. The introduction of C^{α}-tetrasubstituted α-amino acids (Grauer et al. 2009) is a successful way to rigidify the peptide backbone. In particular, (αMe)Val is one of the strongest known helicogenic α-amino acids (Moretto et al. 2008), although its non-methylated counterpart, Val, is a poor helix forming residue. We also analyzed the retro-inverso analogue of **I**. This comparison is theoretically useful because the side chains of the retro-inverso peptide should occupy the same position as the parent peptide, although the backbones are reversed. In this way, it would be possible to study specifically the effect of the side chains orientation. Unfortunately, the retro-inverso analogue of **I** failed to adopt the expected ordered structure in our experimental conditions and it was devoid of any in vivo activity, possibly for this very reason [for more

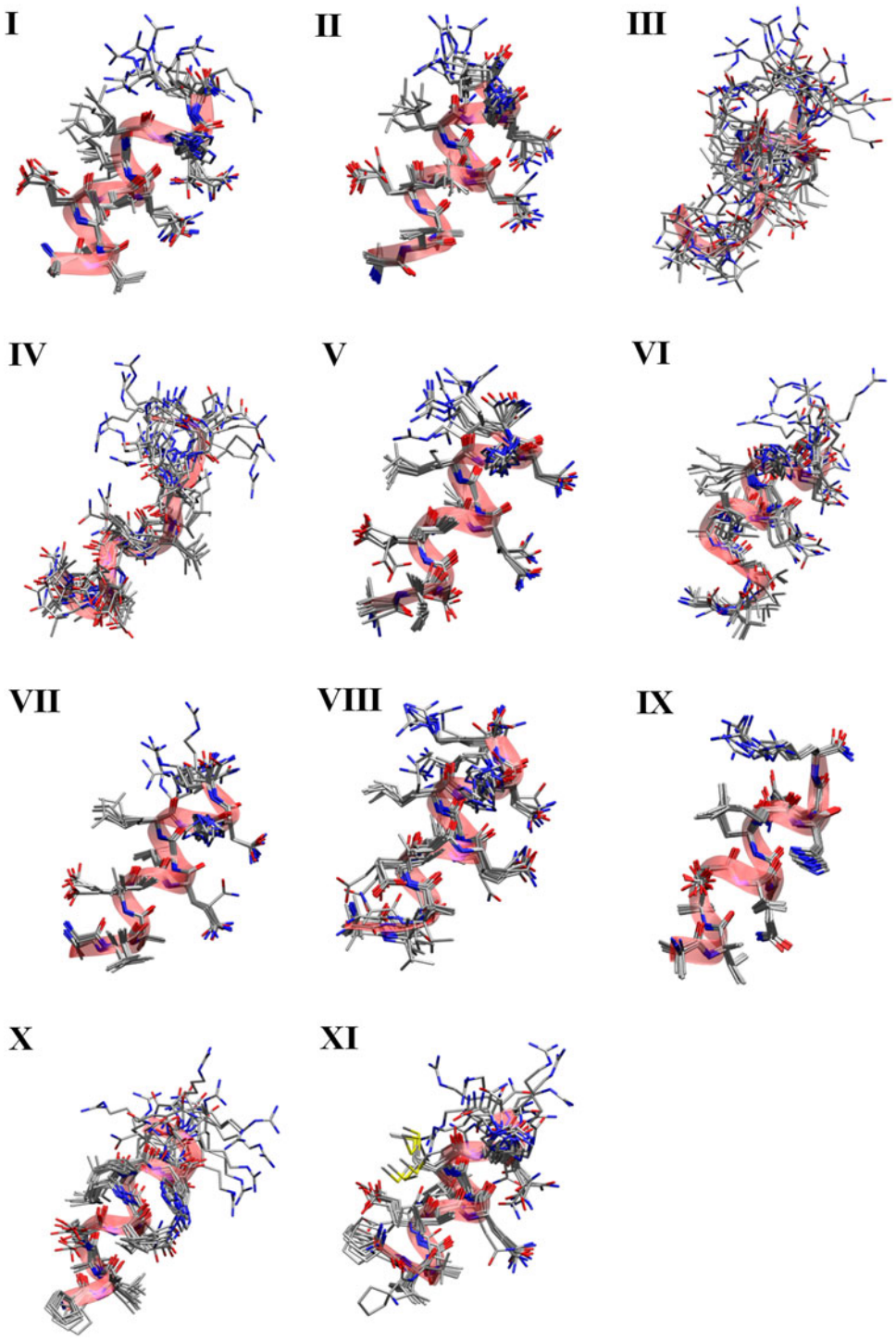

Fig. 3 The overlap of the ten lowest energy structures of all the PTH (1–11) analogues described in this work. Ramachandran plots are reported in the Supporting Information

information, see (Caporale et al. 2009a)]. Nevertheless, we used it as a validation of our model.

The synthesis of analogues containing sterically hindered and helix-promoting C^{α}-tetrasubstituted α-amino acids, such as Aib or (αMe)Val, was carried out by SPPS, using a combination of common solid phase coupling reagents (HBTU/HOBt/DIPEA) and acyl fluoride derivatives, employing Fmoc-protected amino acids. The acyl fluoride coupling method (Wenschuh et al. 1994) was used for its ability to couple sterically hindered α,α-dialkylamino acids, such as Aib, to similarly hindered amino acids. The Fmoc amino acyl fluorides were prepared using cyanuric fluoride, which easily converts amino acids into the corresponding acyl fluorides. They show a better stability toward moisture

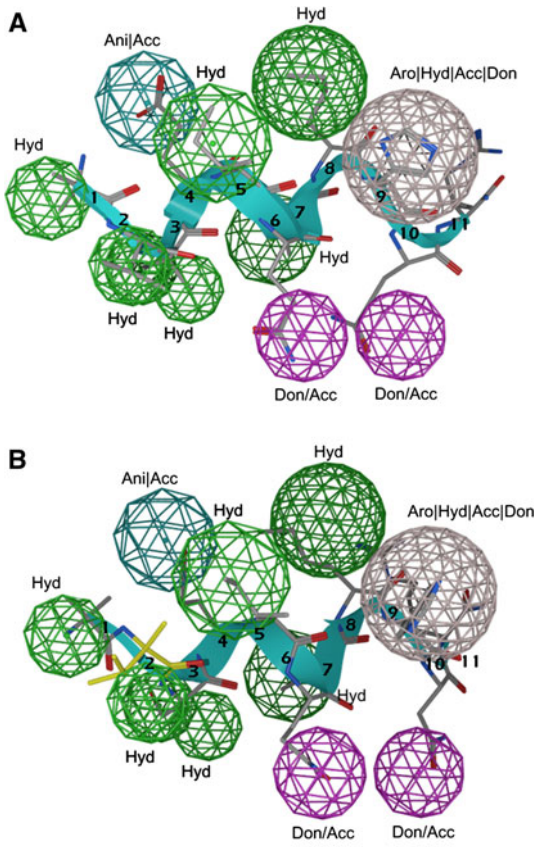

Fig. 4 Analogues **I** and **V** fitting with respect to the pharmacophoric model. The *number* in the *ribbon* refers to the position in the sequence. The *different labels* indicate the different features of each pharmacophoric site represented by the *spheres*. *Hyd* hydrophobic features; *Don/Acc* hydrogen bond donor or acceptor; *Ani/Acc* anionic or hydrogen bond acceptor; *Aro/Hyd/Acc/Don* aromatic/hydrophobic/acceptor/donor. **a** Analogue **I** is aligned into the pharmacophoric model. All the features are fitted in positively by this analogue. **b** The best alignment of **V** (inactive) onto the pharmacophoric model does not result in the fitting of residue Val^2 in the hydrophobic feature, in contrast with analogue **I** in (**a**)

and acid-labile functional groups than acyl chlorides (Carpino et al. 1998; Han and Kim 2004).

With this procedure, a good crude sample was obtained, which was directly observed by mass spectrometry analysis and by analytical HPLC before purification. On the contrary, no correct crude was detectable in mass spectrometry analysis when HATU and HOAt were used as coupling reagents for the same difficult coupling with (αMe)Val. On the other hand, the steric difficulty in the coupling of the first amino acids to the solid support in the synthesis of retro-inverse analogue was resolved using a double coupling method with the HATU/HOAt protocol (Carpino et al. 1995; Caporale et al. 2009a). The replacement of Met^8 with Nle^8 is known to be well tolerated, producing no loss of binding affinity (Rosenblatt et al. 1976), and prevents methionine oxidation, which would result in a decrease of the biological response (Frelinger and Zull 1984).

Only for analogues **IX, X** and **XI**, the CD analysis showed an enhanced or equal ordered structure compared with the reference peptide **I**. The CD shape for analogue **IV** is indicative of a random coil, very near to the zero line; the analogues from **V** to **VIII** show a spectrum shape different from that of a canonical α-helix, with an ellipticity ratio (R) between 222 (the $n \rightarrow \pi^*$ amide transition) and 208 nm (the parallel component of the amide $\pi \rightarrow \pi^*$ transition) lower than 1.0 or very close to 0.6 (see Table S4 in Supporting Information) I.

This behaviour has been attributed to the presence of a right-handed 3_{10}-helix conformation (Polese et al. 1996; Toniolo et al. 2004). Homooligopeptides formed by C^{α}-tetrasubstituted α-amino acids (αMeVal) are the most prone to adopt such conformation, in poor H-bonding donor solvents (Crisma et al. 2007; Hong et al. 1999; Kubasik and Blom 2005; Moretto et al. 2008). Also peptides containing both proteinogenic and C^{α}-tetrasubstituted α-amino acids can display similar effects (e.g., the peptaibol trichogin (Locardi et al. 1998)). In the present case, a single C^{α}-tetrasubstituted α-amino acid is sufficient to elicit such a clear effect in the CD spectrum.

The notable differences among various analogues in terms of biological potency are an indication of the strategic role of Val^2 for the interaction with the PTH1R receptor. Specifically, analogues **I** and **II** differ only for the chirality of Val^2, but the potency of analogue (**II**) is more than three orders of magnitude lower than that of analogue **I** (EC_{50} = 1.1 nM (**I**); $EC_{50} = 7{\cdot}10^3$ nM (**II**)). Also, the simple shift of the side chain from Cα (**I**) to N (**III**) transforms the peptide in an inactive one. The introduction of an αMe group in position 2 preserves the helical structure, but does not prevent the loss of activity in analogues **V–VIII**. Differently, the introduction of Ac_5c in position 1 stabilizes the helix, similarly to Aib, and at the same time keeps Val^2 more correctly oriented (**X–XI**) to activate PTH1R. CD and chemical shift differences indicate the Ac_5c residue as the most effective stabilizer and enhancer of the α-helical structure. The CD spectrum of analogue **XI** has the typical shape of a canonical α-helix, with R close to 1. Also, the ROESY-derived structures of both analogues are similar and mostly α-helical. The only difference between the two analogues is the substitution of Val^2 with (αMe)Val, which causes a dramatic drop in biological potency. All these observations suggest a strict relationship between the activity and side chain orientation of the first residues in the N-terminal portion with respect to the receptor.

Here, we propose a new approach to understand the complex relationship between the structure of PTH (1–11) fragment and its biological role in the activation of PTH1R.

A pharmacophoric model was used to determine the pattern of chemical–physical features that are necessary to promote the receptor activation by active analogues. The goal was to obtain a deeper insight on the structure–activity relationship comparing the ability of the analogues to fit the pharmacophoric model. We have observed that the helix conformation is a requisite for the activity, as it guarantees the correct orientation of the relevant side chains to interact with the receptor. The proposed model identifies a well-defined topology in the N terminus that seems to be fundamental to allow an effective distinction between active analogues and inactive ones (**III**–**VII**). Several hydrophobic sites were detected along the entire helix, underlining the importance of the hydrophobic component in the interaction between PTH (1–11) and PTH1R. The most active compounds show low-RMSD values between the best conformation and the ideal conformation described by the pharmacophoric model (0.8 Å for **I**, 1.38 Å for **XI**), while the less-active compounds have higher RMSD values (1.51 Å for **VIII**; Table S5). All peptides present a good alignment on the features associated with Nle^8 and His^9; on the contrary, the features associated with Glu^4 and with the hydrophobic pattern formed by the first three residues are well described only by the active analogues. The conformational freedom of the N-terminal hydrophobic region is very low, as indicated by the volume of the spheres which describe four of the hydrophobic sites. This observation is in good agreement with the activity variability due to modifications of the first residues. The role of Val^2 is more complex, and a specific orientation of the side chain in the complex between ligand and receptor is required to ensure the activity; the introduction of the methyl substituent on the Cα causes a decrease in the activity, although the peptide maintains a helical conformation (**V–X**). The superposition of these analogues on the model clearly indicates a deviation from optimal orientation of Val^2 that might compromise a hydrophobic contact or produce steric clashes. The possibility that the substantial loss of activity shown by all analogues carrying (αMe)Val in position 2 could be merely determined by the impossibility of accommodating its β-CH_3 substituent within the receptor seems unlikely. Rather, the special disposition of the isopropyl group is significantly altered by the presence of the methyl on the Cα, as can be seen overlapping the structures obtained for the various peptides.

The anionic or hydrogen-bond acceptor feature representing Glu^4 lies on same face of the fundamental residue Nle^8, while the two hydrogen-bond donor/acceptor features of Gln^6 and Gln^{10} are on the opposite side. The orientation of the imidazole ring is well-conserved in all analogues, confirming that the C^{α}-tetrasubtitution on Val^2 does not affect the C-terminal region; the ring extends perpendicularly with respect to Glu^4, Gln^6, Gln^{10}, and Nle^8.

Conclusions

CD, NMR, and MM analyses suggest that the role of Val^2 is critical in the activation of the receptor as it allows the N-terminal segment to adopt a well-defined hydrophobic pattern. The change of chirality of Val^2 (analogue **II**) reduces the potency by three orders of magnitude and the side chain shift from Cα to N (analogue **III**) transforms the peptide in an inactive one. We observed that the 3-D structural order of the canonical helix is not an absolute requirement to produce an enhancement of potency (Barazza et al. 2005). Although the conformational constraints induced by the introduction of C^{α}-tetrasubstituted amino acids, such as Aib or diethylglycine, produce effects on the whole N-terminal segment enhancing its α-helix structure and often the potency (Shimizu et al. 2001a, 2004), the same introduction might result in a conformation with a lower ability to match the appropriate pattern for a productive peptide–receptor interaction. The results are in line with the previous observations on the relationship between the potency and the structure of modified N-terminal analogues of PTH (Monticelli et al. 2002; Dean et al. 2008; Potts and Gardella 2008). According to our present findings, we conclude that the introduction of conformational constraints such as C^{α}-tetrasubstituted amino acids could theoretically represent a useful approach to stabilize a defined helical structure and to reproduce the appropriate pattern for a productive peptide–receptor interaction. However, the real new clue is the recognition of the necessity to obtain a strictly correct spatial orientation of the side chains of the N terminus of the PTH analogues when binding to the receptor. As a result, the activity of the N-terminal segment of PTH is not merely a consequence of helical stabilization, but it also depends on the fitting of specific chemical features. A pharmacophoric description of the side chains can explain how the slight structural modifications lead to notable activity variation. The possibility to obtain structure–activity relationships with atomic resolution has revealed the fundamental role of Val^2 conformation and the consequence of its modification. In addition, this rational approach opens new scenarios in the development of new lead compounds with an improved bioavailability taking advantage of pharmacophoric-based virtual screening.

Acknowledgments The authors thank MIUR, Ministry of Education and University of Italy, for financial support, Dr. Barbara Biondi for her kind help in mass analyses and in the synthetic approach, Dr. Nereo Fiori for his initial NMR analyses and Prof. Stefano Moro and the Molecular Modelling section of the Department of Pharmaceutical Sciences (Padova, Italy) for computational support. In particular, the authors want to thank Prof. Claudio Toniolo for encouragement and helpful discussions. The authors declare that they have no conflict of interest.

References

Baker EN, Hubbard RE (1984) Hydrogen bonding in globular proteins. Prog Biophys Mol Biol 44:97–179

Barazza A, Wittelsberger A, Fiori N, Schievano E, Mammi S, Toniolo C, Alexander JM, Rosenblatt M, Peggion E, Chorev M (2005) Truncation of the carboxyl-terminal region of the rat parathyroid hormone (PTH)-PTH-related peptide receptor enhances PTH stimulation of adenylyl cyclase but not phospholipase C. J Pept Res 65:23–35

Bax A, Davis DG (1985a) Practical aspects of two-dimensional transverse NOE spectroscopy. J Magn Reson 63:207–213

Bax A, Davis DG (1985b) MLEV-17 based two-dimensional homonuclear magnetization transfer spectroscopy. J Magn Reson 65:355–360

Bui TTT, Formaggio F, Crisma M, Monaco V, Toniolo C, Hussain R, Siligardi G (2000) TOAC: a useful C^{α}-tetrasubstituted α-amino acid for peptide conformational analysis by CD spectroscopy in the visible region. Part I. J Chem Soc Perkin Trans 2:1043–1046

Cali JJ, Niles A, Valley MP, O'Brien MA, Riss TL, Shultz J (2008) Bioluminescent assays for ADMET. Expert Opin Drug Metab Toxicol 4:103–120

Caporale A, Fiori N, Schievano E, Mammi S, Peggion E, Chorev M, Wittelsberger A (2006) PTH-like peptides - EP 1619204 A1. US Patent 7,132,394, 25 Jan 2006

Caporale A, Biondi B, Schievano E, Wittelsberger A, Mammi S, Peggion E (2009a) Structure-function relationship studies of PTH (1–11) analogues containing D-amino acids. Eur J Pharmacol 611:1–7

Caporale A, Fiori N, Schievano E, Wittelsberger A, Mammi S, Chorev M, Peggion E (2009b) Structure-function relationship study of parathyroid hormone (1–11) analogues containing D-AA. In: Del Valle S, Escher E, Lubell WD (eds) Peptides for youth. American Peptide Society, Montreal, pp 113–114

Caporale A, Sturlese M, Schievano E, Mammi S, Peggion E (2010a) Synthesis and structural studies of new analogues of PTH (1–11) containing Cα-tetra-substituted amino acids in position 8. Amino Acids 39:1369–1379

Caporale A, Schievano E, Peggion E (2010b) Peptide–peptoid hybrids based on (1–11)-parathyroid hormone analogs. J Pept Sci 16:480–485

Carpino LA, El-Faham A (1994) Effect of tertiary bases on *O*-benzotriazolyluronium salt-induced peptide segment coupling. J Org Chem 59:695–698

Carpino LA, Mansour EME, Sadat-Aalaee D (1991) *tert*-Butyloxycarbonyl and benzyloxycarbonyl amino acid fluorides. New stable rapid-acting acylating agents for peptide synthesis. J Org Chem 56:2611–2614

Carpino LA, El-Faham A, Minor CA, Albericio F (1994) Advantageous applications of azabenzotriazole (triazolopyridine)-based coupling reagents to solid-phase peptide synthesis. J Chem Soc Chem Commun 2:201–203

Carpino LA, El-Faham A, Albericio F (1995) Efficiency in peptide coupling: 1-hydroxy-7-azabenzotriazole versus 3,4-dihydro-3-hydroxy-4-oxo-1,2,3-benzotriazine. J Org Chem 60:3561–3564

Carpino LA, Ionescu D, El-Faham A, Henklein P, Wenschuh H, Bienert M, Beyermann M (1998) Protected amino acid chlorides vs protected amino acid fluorides: reactivity comparisons. Tetrahedron Lett 39:241–244

Castro M, Nikolaev VO, Palm D, Lohse MJ, Vilardaga JP (2005) Turn-on switch in parathyroid hormone receptor by a two-step parathyroid hormone binding mechanism. Proc Natl Acad Sci USA 102:16084–16089

Crisma M, Bonora GM, Toniolo C, Benedetti E, Bavoso A, Di Blasio B, Pavone V, Pedone C (1988) Structural versatility of peptides from Cα,α-dialkylated glycines: an infrared absorption and 1H NMR. study of homopeptides from 1-aminocyclopentane-1-carboxylic acid. J Biol Macromol 10:300–304

Crisma M, Bisson W, Formaggio F, Broxterman QB, Toniolo C (2002) Factors governing 3_{10}-helix vs α-helix formation in peptides: percentage of Cα-tetrasubstituted α-amino acid residues and sequence dependence. Biopolymers 64:236–245

Crisma M, Saviano M, Moretto A, Broxterman QB, Kaptein B, Toniolo C (2007) Peptide $\alpha/3_{10}$ -helix dimorphism in the crystal state. J Am Chem Soc 129:15471–15473

Dean T, Vilardaga JP, Potts JT Jr, Gardella TJ (2008) Altered selectivity of parathyroid hormone (PTH) and PTH-related protein (PTHrP) for distinct conformations of the PTH/PTHrP receptor. Mol Endocrinol 22:156–166

Fan F, Wood KV (2007) Bioluminescent assay for high-throughput screening. Assay Drug Dev Technol 5:127–136

Frelinger AL, Zull JE (1984) Oxidized forms of parathyroid hormone with biological activity. Separation and characterization of hormone forms oxidized at methionine 8 and methionine 18. J Biol Chem 259:5507–5513

Gante J (1994) Peptidomimetics: tailored enzyme inhibitors. Angew Chem Int Ed 33:1699–1720

Gardella TJ, Jüppner H (2001) Molecular properties of the PTH/PTHrP receptor. Trends Endocrinol Metab 5:210–217

Gensure RC, Gardella TJ, Jüppner H (2005) Parathyroid hormone and parathyroid hormone-related peptide, and their receptors. Biochem Biophys Res Commun 328:666–678

Grauer AA, Cabrele C, Zabel M, König B (2009) Stable right- and left-handed peptide helices containing C^{α}-tetrasubstituted α-amino acids. J Org Chem 74:3718–3726

Griesinger C, Otting G, Wüthrich K, Ernst RR (1988) Clean TOCSY for proton spin system identification in macromolecules. J Am Chem Soc 110:7870–7872

Han SY, Kim YA (2004) Recent development of peptide coupling reagents in organic synthesis. Tetrahedron 60:2447–2467

Hirschmann R (1991) Medicinal chemistry in the golden age of biology: lessons from steroid and peptide research. Angew Chem Int Ed 30:1278–1301

Hoare S, Gardella TJ, Usdin T (2001) Evaluating the signal transduction mechanism of the parathyroid hormone 1 receptor: effect of receptor G-protein interaction on the binding mechanism and the receptor conformation. J Biol Chem 276:7741–7753

Hong D-P, Hoshino M, Kuboi R, Goto Y (1999) Clustering of fluorine-substituted alcohols as a factor responsible for their marked effects on proteins and peptides. J Am Chem Soc 121:8427–8433

Hruby VJ, Li G, Haskell-Luevano C, Shenderovich M (1997) Design of peptides, proteins, and peptidomimetics in χ space. Biopolymers 43:219–266

Jüppner H, Abou-Samra AB, Freeman M, Kong XF, Schipani E, Richards J, Kolakowski LF, Hock J, Potts JT, Kronenberg HM, Segre GV (1991) A G-protein-linked receptor for parathyroid hormone and parathyroid hormone-related peptide. Science 254:1024–1026

Kabsch W, Sander C (1983) Dictionary of protein secondary structure: pattern recognition of hydrogen-bonded and geometrical features. Biopolymers 22:2577–2637

Kaul R, Balaram P (1999) Stereochemical control of peptide folding. Bioorg Med Chem 7:105–117

Kessler H, Diefenbach B, Finsinger F, Geyer A, Gurrath M, Goodman SL, Hölzemann G, Haubner R, Jonczyk A, Müller G, Graf von Roedern E, Wermuth J (1995) Design of superactive and selective integrin receptor antagonists containing the RGD sequence. Lett Pept Sci 2:155–160

Kolakowski LF (1994) GCRDb: a G-protein-coupled receptor database. Receptors Channels 2:1–7

Kronenberg H, Abou-Samra A, Bringhurst F, Gardella T, Jüppner H, Segre G (1997) In: Thakker R (ed) Genetics of endocrine and metabolic disorders. Chapman & Hall, London, pp 389–420

Kubasik M, Blom A (2005) Acceleration of short helical peptide conformational dynamics by trifluoroethanol in an organic solvent. ChemBioChem 6:1187–1190

Locardi E, Mammi S, Peggion E, Monaco V, Formaggio F, Crisma M, Toniolo C, Bodo B, Rebuffat S, Kamphuis J, Broxterman Q (1998) Conformation and membrane activity of an analogue of the peptaibol antibiotic trichogin GA IV with a lipophilic amino acid at the N terminus. J Pept Sci 4(6):389–399

Maity P, König B (2008) Enantio- and diastereoselective syntheses of cyclic Cα-tetrasubstituted α-amino acids and their use to induce stable conformations in short peptides. Biopolymers (Pept Sci) 90:8–27

Monticelli L, Mammi S, Mierke DF (2002) Molecular characterization of a ligand-tethered parathyroid hormone receptor. Biophys Chem 95:165–172

Moretto A, Formaggio F, Kaptein B, Broxterman QB, Wu L, Keiderling TA, Toniolo C (2008) First homo-peptides undergoing a reversible 3_{10}-helix/α-helix transition: critical main-chain length. Biopolymers (Pept Sci) 90:567–574

Obrecht D, Bohdal U, Broger C, Bur D, Lehmann C, Ruffieux R, Schönholzer P, Spiegler C, Müller K (1995) L-Phenylalanine cyclohexylamide: a simple and convenient auxiliary for the synthesis of optically pure α,α-disubstituted (R)- and (S)-amino acids. Helv Chim Acta 78:563–580

Perczel A, Hollosi M, Foxman B, Fasman GD (1991) Conformational analysis of pseudocyclic hexapeptides based on quantitative circular dichroism (CD), NOE, and X-ray data. The pure CD spectra of type I and type II beta-turns. J Am Chem Soc 113:9772–9784

Pines M, Adams AE, Stueckle S, Bessalle R, Rashti-Behar V, Chorev M, Rosenblatt M, Suva LJ (1994) Generation and characterization of human kidney cell lines stably expressing recombinant human PTH/PTHrP. Endocrinology 135:1713–1716

Pioszak AA, Parker NR, Gardella TJ, Xu HE (2009) Structural basis for parathyroid hormone-related protein binding to the parathyroid hormone receptor and design of conformation-selective peptides. J Biol Chem 24:28382–28391

Polese A, Formaggio F, Crisma M, Valle G, Toniolo C, Bonora GM, Broxterman QB, Kamphuis J (1996) Peptide helices as rigid molecular rulers: a conformational study of isotactic homopeptides from α-methyl-α-isopropylglycine, $[L\text{-}(\alpha Me)Val]_n$. Chem Eur J 2:1104–1111

Potts JT, Gardella TJ (2008) Progress, paradox, and potential: parathyroid hormone research over five decades. Ann NY Acad Sci 1117:196–208

Rance M, Sørensen OW, Bodenhausen G, Wagner G, Ernst RR, Wüthrich K (1983) Improved spectral resolution in COSY ^{1}H NMR spectra of proteins via double quantum filtering. Biochem Biophys Res Commun 117:479–485

Rosenblatt M, Goltzmann D, Keutmann HT, Tregear GW, Potts JT (1976) Chemical and biological properties of synthetic, sulfur-free analogues of parathyroid hormone. J Biol Chem 251:159–164

Santini A, Barone V, Bavoso A, Benedetti E, Di Blasio E, Fraternali F, Lelj F, Pavone V, Pedone C, Crisma M, Bonora GM, Toniolo C (1988) Structural versatility of peptides from Cα, α-dialkylated glycines: a conformational energy calculation and X-ray diffraction study of homopeptides from 1-aminocyclopentane-1-carboxylic acid. Int J Biol Macromol 10:292–299

Scian M, Marin M, Bellanda M, Tou L, Alexander JM, Rosenblatt M, Chorev M, Peggion E, Mammi S (2006) Backbone dynamics of human parathyroid hormone (1–34): flexibility of the central region under different environmental conditions. Biopolymers 84:147–160

Shimizu M, Potts JT, Gardella TJ (2000) Minimization of parathyroid hormone. Novel amino-terminal parathyroid hormone fragments with enhanced potency in activating the type-1 parathyroid hormone receptor. J Biol Chem 275:21836–21843

Shimizu M, Carter PH, Khatri A, Potts JT, Gardella TJ (2001a) Enhanced activity in parathyroid hormone-(1–14) and -(1–11): novel peptides for probing ligand–receptor interactions. Endocrinology 142:3068–3074

Shimizu N, Guo J, Gardella TJ (2001b) Parathyroid hormone (1–14) and (1–11) analogs conformationally constrained by α-aminoisobutyric acid mediate full agonist responses via the juxtamembrane region of the PTH 1 receptor. J Biol Chem 276:49003–49012

Shimizu N, Shimizu M, Tsang JC, Petroni BD, Khatri A, Potts JT, Gardella TJ (2002) Residue 19 of the parathyroid hormone (PTH) modulates ligand interaction with the juxtamembrane region of the PTH-1 receptor. Biochemistry 41:13224–13233

Shimizu M, Dean T, Khatri A, Gardella TJ (2004) Amino-terminal parathyroid hormone fragment analogs containing α, α-di-alkyl amino acids at positions 1 and 3. J Bone Miner Res 19:2078–2086

Shimizu N, Dean T, Tsang JC, Khatri A, Potts JT, Gardella TJ (2005) Novel parathyroid hormone (PTH) antagonists that bind to the juxtamembrane portion of the PTH/PTH-related protein receptor. J Biol Chem 280:1797–1807

Toniolo C (1989) Structure of conformationally constrained peptides: from model compounds to bioactive peptides. Biopolymers 28:247–257

Toniolo C, Polese A, Formaggio F, Crisma M, Kamphuis J (1996) Circular dichroism spectrum of a peptide 310-helix. J Am Chem Soc 118:2744–2745

Toniolo C, Crisma M, Formaggio F, Peggion C (2001) Control of peptide conformation by the Thorpe–Ingold effect (C^{α}-tetrasubstitution). Biopolymers (Pept Sci) 60:396–419

Toniolo C, Formaggio F, Tognon S, Broxterman QB, Kaptein B, Huang R, Setnicka V, Keiderling TA, McColl IH, Hecht L, Barron LD (2004) The complete chirospectroscopic signature of the peptide 310-helix in aqueous solution. Biopolymers 75:32–45

Torras J, Zanuy D, Crisma M, Toniolo C, Betran O, Alemán C (2008) Correlation between symmetry breaker position and the preferences of conformationally constrained homopeptides: a molecular dynamics investigation. Biopolymer (Pept Sci) 90:695–706

Tsomaia N, Pellegrini M, Hyde K, Gardella TJ, Mierke DF (2004) Toward parathyroid hormone minimization: conformational studies of cyclic PTH (1–14) analogues. Biochemistry 43:690–699

Vilardaga JP, Romero G, Friedman PA, Gardella JT (2011) Molecular basis of parathyroid hormone receptor signalling and trafficking: a family B GPCR paradigm. Cell Mol Life Sci. doi:10.1007/s00018-010-0465-9

Wenschuh H, Beyermann M, Krause E, Brudel M, Winter R, Schümann M, Carpino LA, Bienert M (1994) Fmoc amino acid fluoride: convenient reagents for the solid-phase assembly of peptides incorporating sterically hindered residues. J Org Chem 59:3275–3280

Willisch H, Hiller W, Hemmasi B, Bayer E (1991) Synthesis, properties and crystal structure of the tripeptide boc-L-prolyl-L-propargylglycyl-glycine methylester. Tetrahedron 47:3947–3958

Wittelsberger A, Corich M, Thomas BE, Lee BK, Barazza A, Czodrowski P, Mierke DF, Chorev M, Rosenblatt M (2006) The mid region of parathyroid hormone (1–34) serves as functional docking domain in receptor activation. Biochemistry 45:2027–2034

Wüthrich K (1986) NMR of proteins and nucleic acids. Wiley, Weinheim

Yang JT, Wu CS, Martinez HM (1986) Calculation of protein conformation from circular dichroism. Methods Enzymol 130:208–269